Suppression of renal cell carcinoma growth by inhibition of Notch signaling in vitro and in vivo

Jonas Sjölund,[1] Martin Johansson,[1] Sugata Manna,[1] Carl Norin,[1] Alexander Pietras,[1] Siv Beckman,[1] Elise Nilsson,[1] Börje Ljungberg,[2] and Håkan Axelson[1]

[1]Center for Molecular Pathology, Department of Laboratory Medicine, Lund University, University Hospital MAS, Malmö, Sweden.
[2]Department of Surgical and Perioperative Sciences and Department of Urology and Andrology, Umeå University, Umeå, Sweden.

Loss of the tumor suppressor gene von Hippel–Lindau (*VHL*) plays a key role in the oncogenesis of clear cell renal cell carcinoma (CCRCC). The loss leads to stabilization of the HIF transcription complex, which induces angiogenic and mitogenic pathways essential for tumor formation. Nonetheless, additional oncogenic events have been postulated to be required for the formation of CCRCC tumors. Here, we show that the Notch signaling cascade is constitutively active in human CCRCC cell lines independently of the VHL/HIF pathway. Blocking Notch signaling resulted in attenuation of proliferation and restrained anchorage-independent growth of CCRCC cell lines. Using siRNA targeting the different Notch receptors established that the growth-promoting effects of the Notch signaling pathway were attributable to Notch-1 and that Notch-1 knockdown was accompanied by elevated levels of the negative cell-cycle regulators $p21^{Cip1}$ and/or $p27^{Kip1}$. Treatment of nude mice with an inhibitor of Notch signaling potently inhibited growth of xenotransplanted CCRCC cells. Moreover, Notch-1 and the Notch ligand Jagged-1 were expressed at significantly higher levels in CCRCC tumors than in normal human renal tissue, and the growth of primary CCRCC cells was attenuated upon inhibition of Notch signaling. These findings indicate that the Notch cascade may represent a novel and therapeutically accessible pathway in CCRCC.

Introduction

Each year, renal cell carcinoma (RCC) afflicts about 150,000 people globally and accounts for nearly 78,000 deaths (1). Although recent years have yielded important information about the underlying molecular mechanisms of renal oncogenesis, nephrectomy still remains the basis of treatment for RCCs. Accordingly, effective therapy for patients with metastatic advanced-stage RCC is limited, though recent data show that treatment with multikinase inhibitors significantly prolongs progression-free survival (2, 3).

Clear cell RCC (CCRCC), which accounts for approximately 75% of all RCCs, is characterized by inactivation of the von Hippel–Lindau (*VHL*) tumor suppressor gene (1). Reintroduction of functional VHL protein (pVHL) into *VHL*-negative CCRCC cells totally suppressed their capacity to form tumors in nude mice (4). The tumor suppressive function of pVHL has been attributed to its role in a multiprotein complex that targets the α-subunits of the HIFs (HIF-1α and HIF-2α) for degradation in an oxygen-dependent manner (5–7). HIF-1α and HIF-2α are transcription factors that are instrumental in cellular responses to hypoxia. Loss of pVHL leads to oxygen-independent stabilization of HIF-α subunits and upregulation of a diverse range of HIF targets that regulate metabolism, glucose transport, proliferation, and angiogenesis (8). Of the 2 HIF-α isoforms, HIF-2α is the key mediator in the tumorigenic process of CCRCCs (5), most likely due to different functional characteristics of the HIF-α proteins (9–11). Clearly, HIF-α stabilization is instrumental in tumor formation, but based on genetic and molecular studies, it has been postulated that unknown additional tumorigenic events are required for the genesis of CCRCCs (12, 13).

Notch signaling is critical for determination of cell fates within a wide variety of tissues by regulation of growth, differentiation, and apoptosis. The 4 mammalian Notch receptors (Notch-1 to Notch-4) are single-pass, heterodimeric transmembrane proteins that serve as receptors for the Delta-like (Dll-1, Dll-3, and Dll-4) and Jagged (Jagged-1 and Jagged-2) ligands expressed on neighboring cells (14). Ligand binding leads to 2 subsequent proteolytic cleavages that release the intracellular domain of Notch (icNotch), which then transits to the nucleus, where it converts the transcriptional repressor CBF1/suppressor of hairless/Lag-1 to an activator (15). The principal transcriptional outputs of the Notch cascade are a set of basic helix-loop-helix factors of the hairy and enhancer of split (Hes) and Hes-related repressor protein (Hey) families (16). Importantly, the second cleavage is mediated by the γ-secretase complex, and effective inhibition of Notch activation can be achieved using pharmacological inhibitors of this proteolytic activity. The association between dysregulation of the Notch pathway and human cancer is firmly established in T cell acute lymphoblastic leukemias, in which point mutations or chromosomal translocations of the *Notch-1* receptor lead to constitutive signaling (17, 18). Accumulating data indicate that dysregulated Notch activity is also involved in the genesis of other human cancers, such as melanoma, glioma, breast cancer, pancreatic cancer,

Nonstandard abbreviations used: CCRCC, clear cell renal cell carcinoma; CDK, cyclin-dependent kinase; DAPT, *N*-[*N*-(3,5-difluorophenacetyl)-L-alanyl]-*S*-phenylglycine *t*-butyl ester; Dll, Delta-like ligand; Hes, hairy and enhancer of split; Hey, Hes-related repressor protein; icNotch, intracellular Notch; L-685458, (5S)-(t-butoxycarbonylamino)-6-phenyl-(4R)hydroxy-(2R)benzylhexanoyl)-L-leu-L-phe-amide; PCNA, proliferating cell nuclear antigen; PEST, penicillin/streptomycin; PI, propidium iodide; pVHL, VHL protein; Q-PCR, quantitative real-time PCR; RCC, renal cell carcinoma; TB, trypan blue; VHL, von Hippel–Lindau.

Conflict of interest: The authors have declared that no conflict of interest exists.

Citation for this article: *J. Clin. Invest.* **118**:217–228 (2008). doi:10.1172/JCI32086.

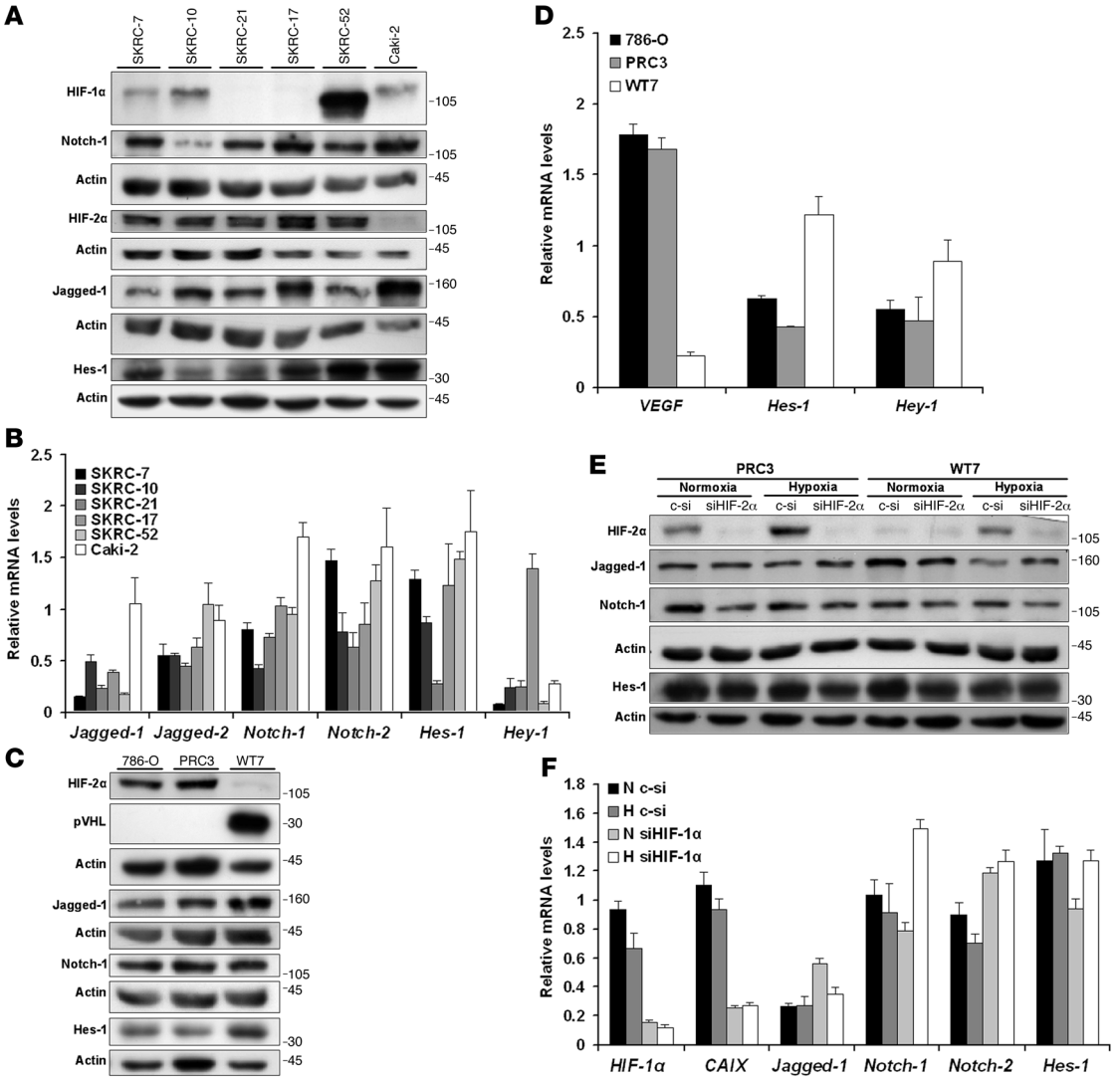

Figure 1

Notch signaling pathway components are expressed in CCRCC cells and maintained in a HIF-1α– and HIF-2α–independent manner. (**A**) Immunoblots of SKRC-7, SKRC-10, SKRC-21, SKRC-17, SKRC-52, and Caki-2 cell lysates analyzed for indicated proteins. Actin was used as a control for equal loading of samples. (**B**) Q-PCR analyses of *Jagged-1*, *Jagged-2*, *Notch-1*, *Notch-2*, *Hes-1*, and *Hey-1* mRNA expression in CCRCC cells. mRNA levels were normalized to succinate dehydrogenase complex subunit A (*SDHA*), tyrosine 3-monooxygenase/tryptophan 5-monooxygenase activation protein (*YWHAZ*), and ubiquitin C (*UBC*) expression. Data shown are mean + SD of representative experiment performed in triplicate. (**C**) 786-O, PRC3, and WT7 cell lysates were analyzed for pVHL, HIF-2α, Jagged-1, Notch-1, and Hes-1 expression by Western blot analyses. (**D**) *VEGF*, *Hes-1*, and *Hey-1* mRNA levels in WT7, PRC3, and 786-O cells. Data shown are mean + SD of representative experiment performed in triplicate. (**E**) PRC3 and WT7 cells, transfected with control (c-si) or *HIF-2α* siRNA (siHIF-2α) for 6 hours and then incubated under either normoxic (21% O_2) or hypoxic (1% O_2) conditions for 24 hours prior to protein extract preparation, were subjected to immunoblotting of indicated proteins. (**F**) Q-PCR analyses of indicated mRNAs following control or *HIF-1α* siRNA (siHIF-1α) transfection of SKRC-10 cells. Treatment procedure (N, normoxia; H, hypoxia) and transfection were performed as indicated in **E**. Data shown are mean + SD of representative experiment performed in triplicate.

medulloblastoma, and colorectal, cervical, and mucoepidermoid carcinomas (19, 20). In these tumors, the oncogenic effect of Notch signaling reflects an aberrant recapitulation of the highly tissue-specific function of the cascade during normal development and in tissue homeostasis, where, in most cases, active Notch signaling maintains the cells in an immature, proliferating state.

There are several recent studies showing that the Notch signaling pathway has an important role during development of the mammalian kidney. Several key members of the Notch cascade are expressed during nephrogenesis (21). Inhibition of Notch signaling results in a decrease of the epithelial compartment within the developing mouse kidney, with a particular reduction of the proximal tubules (22), the tissue from which CCRCC is thought to arise (23). Furthermore, targeted mutation of *Notch-2* in mice leads to severe defects in kidney development (24, 25).

Hypoxia attenuates differentiation of muscle and neuronal progenitor cells in a Notch-dependent manner. These observations were explained by the finding that HIF-1α interacts with icNotch-1

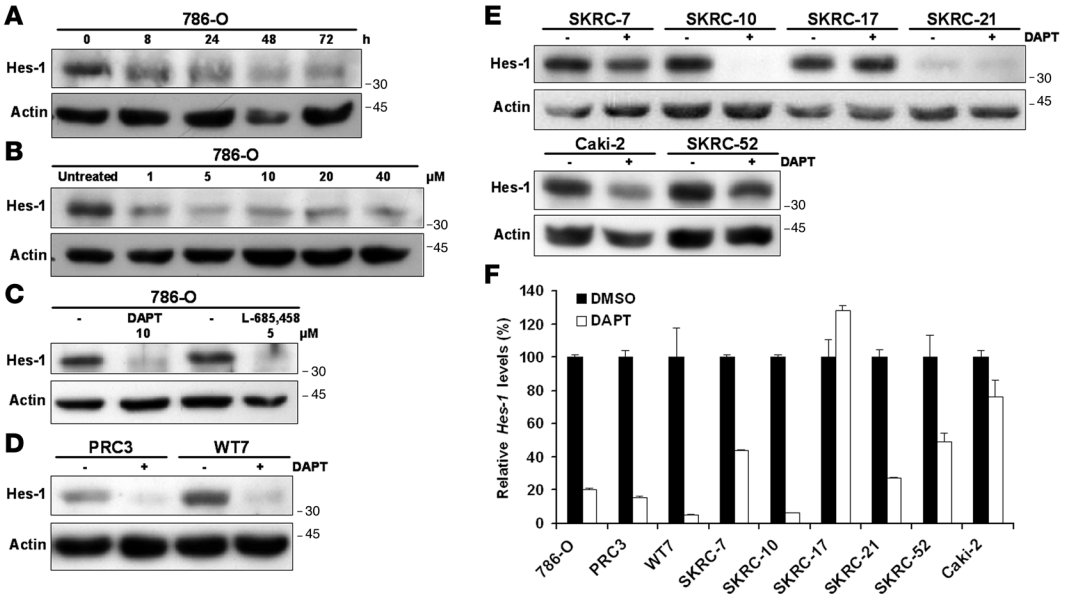

Figure 2

The Notch signaling pathway is active in CCRCC cells. (**A**) Inhibition of the Notch signaling pathway in 786-O cells with a single concentration (10 μM) of the γ-secretase inhibitor DAPT for indicated time periods as monitored by Hes-1 levels. Cells were harvested at indicated time points, and cell lysates were analyzed by immunoblotting. (**B**) Inhibition of the Notch signaling pathway in 786-O cells with increasing concentrations of the γ-secretase inhibitor DAPT for 24 hours. Immunoblotting experiments to measure expression levels of the Notch target Hes-1. (**C**) The effects of L-685458 and DAPT on Hes-1 protein levels in 786-O cells treated for 24 hours compared with DMSO-treated (–) cells. (**D**) DAPT (+) treatment compared with vehicle control (–) treatment of PRC3 and WT7 cells. Cells were harvested after 24 hours of treatment, and cell lysates were analyzed for Hes-1 protein expression. (**E**) DAPT (+) treatment compared with vehicle control (–) treatment in a panel of CCRCC cells. Cells were harvested after 24 hours of treatment, and cell lysates were analyzed for Hes-1 protein expression. (**F**) *Hes-1* mRNA levels assessed by Q-PCR in DAPT-treated CCRCC cells. Cells were harvested after 24 hours of treatment. DMSO-treated samples were designated as 100%, and data shown are mean + SD of representative experiment performed in triplicate.

and enhances the expression of Notch target genes (26). Furthermore, we have shown that Notch signaling is elevated in hypoxic neuroblastoma cells, which might contribute to the immature phenotype of this tumor (27, 28).

In light of the important function of Notch signaling in renal development, in combination with studies showing a crosstalk between the Notch and VHL/HIF pathways, we investigated the role of Notch signaling in CCRCC. Our results show that the components of the Notch pathway are expressed and active in CCRCC independent of the function of VHL and that Notch inhibition perturbs growth of CCRCC cells in vitro. Importantly, we could show that intermittent treatment with a γ-secretase inhibitor effectively inhibited CCRCC tumor growth in vivo and that this treatment regime minimized the well-known adverse effect on goblet cell differentiation associated with systemic Notch inhibition. Together, these results show that the Notch pathway might represent a previously unappreciated therapeutic opportunity for treatment of CCRCCs.

Results

Notch signaling pathway components are expressed in CCRCC cells. To address whether CCRCC cells express Notch signaling components, we performed Western blot experiments using extracts from a panel of CCRCC cell lines. The cell lines investigated expressed either HIF-2α only (SKRC-21, SKRC-17) or both HIF-1α and HIF-2α (SKRC-7, SKRC-10, SKRC-52), as shown in Figure 1A and as previously reported (29). The CCRCC cell line Caki-2, which expresses wild-type pVHL (30), did not express HIF-2α. Low expression of HIF-1α was, for unknown reasons, however, detected in this cell line, as reported elsewhere (30). Jagged-1 and Notch-1 expression was detected in all cell lines investigated. Furthermore, expression of the primary Notch downstream target Hes-1 was detected at varying levels in all cell lines examined (Figure 1A). It should be noted that 2 of the cell lines (SKRC-17 and SKRC-52) are derived from metastatic lesions (31). Using quantitative real-time PCR (Q-PCR), we detected expression of *Jagged-1*, *Jagged-2*, *Notch-1*, *Notch-2*, *Hes-1*, and *Hey-1* mRNAs in all cell lines investigated (Figure 1B), while the expression of *Dll-1, Dll-3, Notch-3*, and *Hey-2* was below detection. Taken together, these results show that the expression of Notch ligands, receptors, and downstream targets is a general characteristic of CCRCC cells, seemingly independent of both VHL status and expression of either of the 2 HIF-α isoforms.

Expression of Notch signaling components is independent of VHL, HIF-1α, and HIF-2α expression. To further clarify whether the Notch cascade is expressed independently of the VHL/HIF axis, we employed the *VHL*-negative CCRCC cell line 786-O and subclones transfected with empty (PRC3) or *VHL*-expressing vector (WT7), which have been extensively studied with regard to the tumor suppressor function of pVHL, both in vivo and in vitro (4, 5). As previously reported (7), the 786-O and PRC3 cells expressed high levels of HIF-2α due to the absence of pVHL, while no expression could be detected in the WT7 cells (Figure 1C). The Notch-1 receptor was expressed at equal levels in 786-O, PRC3, and WT7 cells (Figure 1C). Expression of Jagged-1 and Hes-1 was readily detected in the 786-O and PRC3 cells, and a modest elevation of the expression

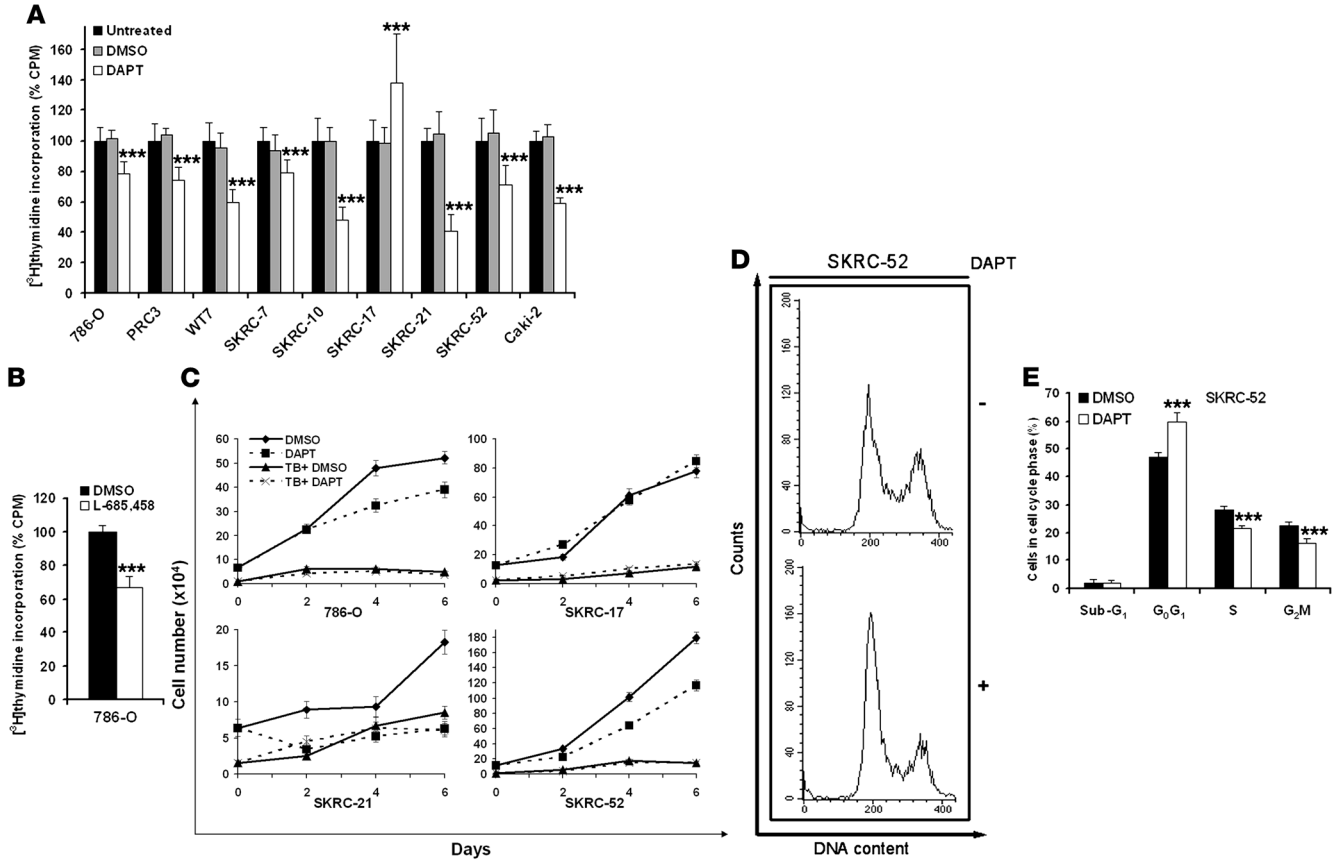

Figure 3

Inhibition of Notch signaling impairs growth of CCRCC cells. (**A**) [^{3}H]thymidine incorporation of a panel of CCRCC cells treated for 72 hours with DMSO or DAPT or left untreated (100%). The bars represent mean + SD of 3 independent experiments, each performed 6 times. ***$P < 0.001$, statistically significant changes (DAPT versus DMSO). (**B**) 786-O cells treated for 72 hours with DMSO or the alternate γ-secretase inhibitor L-685458 and then analyzed for [^{3}H]-thymidine incorporation. The bars represent mean + SD of 3 independent experiments, each performed 6 times. L-685458–treated cells were normalized to DMSO-treated cells. ***$P < 0.001$, statistically significant changes (L-685458 versus DMSO). (**C**) The number of viable (diamonds, DMSO; squares, DAPT) and dead cells (triangles, TB$^+$ DMSO; x's, TB$^+$ DAPT) was determined by TB exclusion experiments at indicated times in a panel of CCRCC cells treated with DMSO or DAPT. Results expressed as mean ± SEM of 1 representative experiment performed in triplicate. (**D** and **E**) Cell-cycle distribution examined by PI staining and flow cytometry of SKRC-52 cells synchronized by serum starvation and treated with DMSO or DAPT for 24 hours. Results visualized as representative experiment (**D**) or mean + SD of 3 experiments (**E**), each performed in triplicate. ***$P < 0.001$, statistically significant changes (DAPT versus DMSO).

was detected in the pVHL-reconstituted WT7 cells (Figure 1C). To exclude clonal variations of the PRC3 and WT7 cells, a series of independent pVHL-reconstituted clones were analyzed by immunoblotting, verifying that Hes-1 expression was not substantially affected by presence or absence of pVHL (data not shown). Q-PCR analyses confirmed that the established HIF target gene *VEGF* was expressed at substantially lower levels in the WT7 clone expressing pVHL compared with the control clone and 786-O (Figure 1D). Furthermore, the expression of the Notch target genes *Hes-1* and *Hey-1* was elevated in pVHL-reconstituted cells. Thus, reexpression of pVHL does not correlate with a marked decrease of Notch signaling, which would have been expected if a HIF-mediated potentiation of Notch signaling, as reported in other cell systems (26), were at hand in CCRCC cells.

It is known that HIF-α transcriptional activity is regulated by oxygen-dependent hydroxylation of the transactivating domain by FIH-1 (12, 32). We therefore also compared the expression of the Notch signaling components in PRC3 and WT7 cells at normoxia and hypoxia in order to elucidate whether an effect on this pathway could be detected in a hypoxic context. In addition, we also ablated *HIF-2α* expression using siRNA in this experimental setup. We could confirm the efficacy of the siRNA in both clones and the restoration of the hypoxic response in WT7 cells (Figure 1E). No substantial differences in expression of Jagged-1, Notch-1, and Hes-1 could be detected, irrespective of the oxygenation status of the cells or the absence or presence of HIF-2α (Figure 1E). Since 786-O cells and the derivative clones only express HIF-2α (7), we also assessed the effect of *HIF-1α* knockdown at normoxia and hypoxia in the SKRC-10 cell line, which expresses both HIF-1α and HIF-2α (Figure 1A). While the HIF-1α target carbonic anhydrase IX (*CAIX*) (29) clearly was downregulated in cells transfected with siRNA directed against *HIF-1α* in comparison with control-transfected cells (Figure 1F), no consistent negative effect on the expression of Notch pathway components could be detected upon *HIF-1α* ablation or hypoxic culturing conditions. Taken together, these experiments clearly establish that Notch signaling in CCRCC cells

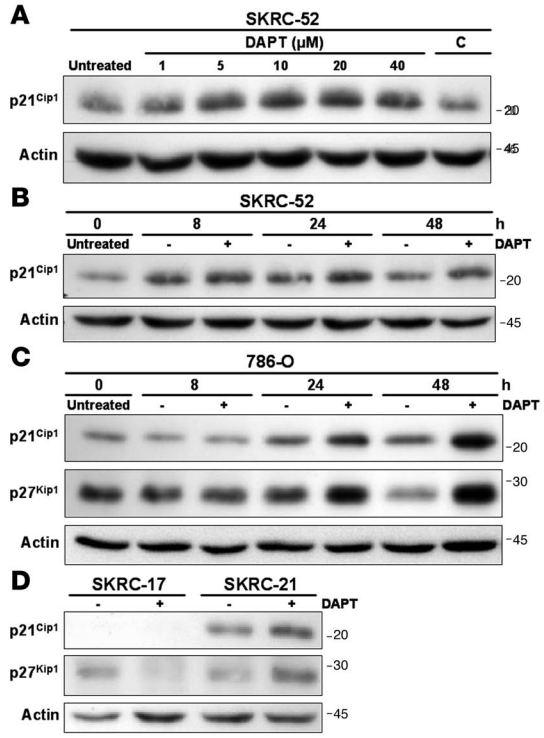

Figure 4
Notch inhibition of CCRCC cells results in elevation of $p21^{Cip1}$ and/or $p27^{Kip1}$ proteins. (**A**) Immunoblotting with a $p21^{Cip1}$ antibody of lysates from SKRC-52 cells treated with increasing concentrations of the γ-secretase inhibitor DAPT. Cells were grown in medium containing 1% FCS. DAPT- and vehicle control–treated cells were harvested after 24 hours of stimulation (C, volume of DMSO corresponding to 40 μM DAPT). (**B**) Immunoblotting of $p21^{Cip1}$ after γ-secretase (+) or control (–) treatment of SKRC-52 cells. Cells were harvested at indicated time points. (**C**) Immunoblotting of $p21^{Cip1}$ and $p27^{Kip1}$ after γ-secretase (+) or control (–) treatment of 786-O cells. Cells were harvested at indicated time points. (**D**) $p21^{Cip1}$ and $p27^{Kip1}$ Western blot analyses of lysates from SKRC-17 and SKRC-21 cells treated for 48 hours with γ-secretase (+) or vehicle control (–).

is maintained in a HIF-1α– and HIF-2α–independent manner, irrespective of the oxygenation status of the cells.

The Notch signaling cascade is active in CCRCC cells. We next sought to experimentally verify that the Notch pathway is active in CCRCC cells. Induction of Notch signaling is based on the activity of the γ-secretase complex. Chemical compounds that specifically inhibit this proteolytic activity have been extensively used for experimental studies of Notch signaling, both in vitro and in vivo (33). CCRCC cells were therefore treated with the Notch inhibitor *N*-[*N*-(3,5-difluorophenacetyl)-L-alanyl]-*S*-phenylglycine *t*-butyl ester (DAPT), and the expression of the Notch target Hes-1 was monitored using Western blot analyses. As shown in Figure 2A, treatment of 786-O cells with DAPT led to a prominent Hes-1 downregulation already after 8 hours, and this effect was maintained for at least 72 hours. Furthermore, treatment of 786-O cells with increasing concentrations led to a dose-dependent decrease of Hes-1 (Figure 2B). We could also show that treatment with the chemically distinct (33) γ-secretase inhibitor (5S)-(t-butoxycarbonylamino)-6-phenyl-(4R)hydroxy-(2R)benzylhexanoyl)-L-leu-L-phe-amide (L-685458) led to a dramatic downregulation of Hes-1 in 786-O cells (Figure 2C). The effect of DAPT treatment was independent of the pVHL status of the cells, as the efficacy of Hes-1 downregulation was equal in PRC3 and WT7 cells (Figure 2D). In order to further establish that active Notch signaling is a common feature of CCRCC cells, we assessed the effect of DAPT treatment on Hes-1 expression in the additional cell lines included in this study. The SKRC-7, SKRC-10, SKRC-21, Caki-2, and SKRC-52 cells also responded to γ-secretase treatment, albeit the extent of Hes-1 downregulation varied among the cell lines (Figure 2E). However, the Hes-1 protein level in SKRC-17 cells was not affected by DAPT treatment (Figure 2E), suggesting that this particular cell line, for unknown reasons, was insensitive to γ-secretase inhibition. Q-PCR experiments showed that the downregulation of *Hes-1* in the DAPT-responsive cell lines occurred at the transcriptional level (Figure 2F). Together, these data show that the Notch signaling cascade is active in a wide range of CCRCC cell lines.

Inhibition of Notch signaling attenuates CCRCC growth. Prior studies have shown that active Notch signaling contributes to cellular proliferation in a distinct set of tumor cell types (20). Hence, treatment with γ-secretase inhibitors attenuates the growth capacity of these tumor cells. We therefore treated the various CCRCC cell lines with DAPT and evaluated the rates of cellular proliferation by means of [^{3}H]thymidine incorporation. In all cell lines, [^{3}H]thymidine incorporation was significantly reduced upon treatment with DAPT compared with vehicle control (Figure 3A), with the exception of the SKRC-17 cell line, which, in contrast, responded with a significant increase in proliferation upon treatment. The observation that DAPT treatment did not negatively affect proliferation of SKRC-17 indicates that the drug did not have a general toxic effect on CCRCC cells. To further exclude the possibility of nonspecific toxic effects of DAPT, 786-O cells were treated with the γ-secretase inhibitor L-685458. A significant reduction in proliferation was also noted using this inhibitor (Figure 3B). To further assess the effect on proliferation, we performed trypan blue (TB) exclusion experiments. As shown in Figure 3C and Supplemental Figure 1 (supplemental material available online with this article; doi:10.1172/JCI32086DS1), DAPT treatment of CCRCC cells led to a decrease in the number of viable cells detectable after 2 to 4 days in culture. In line with previous data, SKRC-17 cells were not negatively affected by γ-secretase inhibition. Since treatment with DAPT did not substantially affect the number of TB-positive cells (Figure 3C) compared with vehicle-treated cells, our data indicate that the decreased number of cells upon Notch inhibition was not due to increased cell death. This notion was corroborated using annexin V/propidium iodide (PI) staining (data not shown). Together, these results indicated that γ-secretase treatment was associated with a block in cell-cycle progression and not increased apoptosis. We therefore performed PI staining and flow cytometry to define the arrest pattern of DAPT-treated SKRC-52 cells. A significant increase of cells in G_0G_1, rising from 47% to 60%, was detected upon treatment (Figure 3, D and E). We conclude that active Notch signaling might be important for progression beyond the G_1 stage in the cell cycle. Furthermore, the sub-G_1 fraction containing apoptotic or necrotic cells was not affected by DAPT treatment (Figure 3E).

Notch inhibition leads to elevation of $p21^{Cip1}$ and/or $p27^{Kip1}$. To further characterize the G_0G_1 arrest, we assayed the expression of cell-cycle regulatory factors associated with Notch signaling activity. No significant effect on the levels of *c-myc*, p53, *Skp-2*, and *cyclin D1* (34–37)

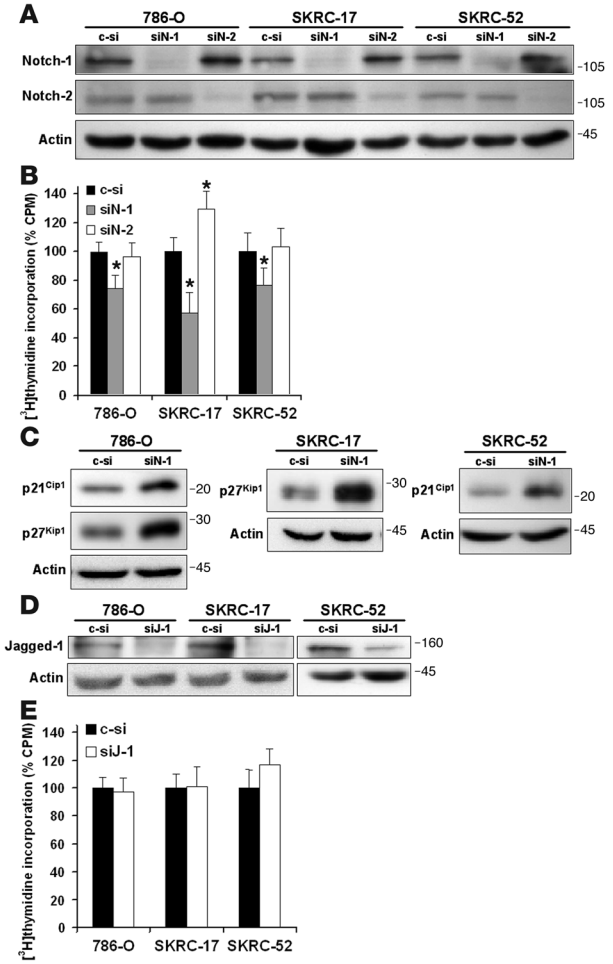

Figure 5
Ablation of endogenous *Notch-1* by siRNA attenuates growth of CCRCC cells and is associated with elevation of $p21^{Cip1}$ and/or $p27^{Kip1}$. (**A**) Inhibition of Notch-1 and Notch-2 protein expression in CCRCC cells employing siRNA. 786-O, SKRC-17, and SKRC-52 cells were transfected either with nonspecific control, *Notch-1*–specific (siN-1), or *Notch-2*–specific (siN-2) siRNAs. Cells were harvested after 24 hours of transfection, and cell lysates were analyzed for Notch-1 and Notch-2 protein expression. (**B**) [^{3}H]thymidine incorporation of 786-O, SKRC-17, and SKRC-52 cells following siRNA transfection for 24 hours and incubation for 72 hours. Bars represent mean + SD of 3 independent experiments, each performed with each transfection 6 times. *Notch-1*–specific (siN-1) and *Notch-2*–specific (siN-2) siRNA-transfected cells were normalized to nonspecific control-transfected cells. *$P < 0.001$, statistically significant changes (siN-1 versus c-si or siN-2 versus c-si). (**C**) Western blotting of $p21^{Cip1}$ and/or $p27^{Kip1}$ in 786-O, SKRC-17, or SKRC-52 cells transfected with either nonspecific control or *Notch-1*–specific siRNA. The cells were transfected for 24 hours and harvested after another 24 hours. (**D**) Knockdown of Jagged-1 employing *Jagged-1*–specific (siJ-1) siRNA. 786-O, SKRC-17, and SKRC-52 cells were transfected with either nonspecific control or *Jagged-1*–specific siRNAs. Cells were harvested after 24 hours of transfection, and cell lysates were analyzed for Jagged-1 and actin protein expression. (**E**) [^{3}H]-thymidine incorporation of CCRCC cells following control or *Jagged-1* siRNA transfection for 24 hours and incubation for 72 hours. Bars represent mean + SD of 3 independent experiments, each performed with each transfection 6 times. *Jagged-1*–specific siRNA-transfected cells were normalized to nonspecific control-transfected cells.

could be detected in CCRCC cells treated with DAPT or in siRNA transfection experiments (data not shown). We next focused on the cyclin-dependent kinase (CDK) inhibitors $p21^{Cip1}$ and $p27^{Kip1}$, previously linked to Notch-associated growth promotion (38, 39). Notch inhibition had no substantial effect on the expression of these cell-cycle regulators at the transcriptional level (data not shown). However, a dose- and time-dependent increase in $p21^{Cip1}$ protein levels was detected when SKRC-52 cells were treated with DAPT (Figure 4, A and B). The level of $p27^{Kip1}$ was below detection in this cell line. Also, in 786-O cells, an accumulation of $p21^{Cip1}$ was detected upon Notch inhibition in a time-course experiment (Figure 4C). A considerable accumulation of $p27^{Kip1}$ protein was further detected in 786-O cells in these experiments (Figure 4C). SKRC-21 cells responded to DAPT treatment with an upregulation of both $p21^{Cip1}$ and $p27^{Kip1}$ (Figure 4D). In contrast, the DAPT refractory SKRC-17 cell line expressed no detectable $p21^{Cip1}$, while the $p27^{Kip1}$ level decreased upon treatment with the γ-secretase inhibitor (Figure 4D). Our findings argue that one mechanism by which Notch signaling promotes growth of CCRCC cells is by suppression of $p21^{Cip1}$ and/or $p27^{Kip1}$.

Notch-1 ablation inhibits CCRCC proliferation and leads to elevation of $p21^{Cip1}$ and/or $p27^{Kip1}$. Our expression analyses showed that CCRCC cells express appreciable levels of Notch-1 and Notch-2 receptors, which are both sensitive to inhibition by the general pathway blocker DAPT. In addition, it remains possible that DAPT mediated its effects on CCRCC cells through γ-secretase–dependent targets other than the Notch receptors (40). We therefore targeted each of the 2 receptors using siRNA in order to elucidate their respective contribution to proliferation. 786-O, SKRC-17, and SKRC-52 cells were transfected with siRNAs directed against *Notch-1* or *Notch-2*. The efficacy and specificity of respective siRNA was confirmed using Western blotting (Figure 5A). We next measured proliferation after transfection with siRNA using [^{3}H]thymidine incorporation assays. *Notch-1* ablation led to a significant decrease in proliferation compared with control siRNA in all 3 cell lines tested, including the γ-secretase–insensitive SKRC-17 cell line (Figure 5B). In contrast, no effect on cell proliferation could be detected in 786-0 and SKRC-52 cells upon ablation of *Notch-2* expression, while SKRC-17 cells responded with increased proliferation.

We next asked whether the growth inhibitory effect of *Notch-1* knockdown was associated with increased expression of $p21^{Cip1}$ and/or $p27^{Kip1}$ in analogy with the effects of DAPT treatment. In 786-O cells, a clear accumulation of both $p21^{Cip1}$ and $p27^{Kip1}$ could be detected when Notch-1 expression was ablated (Figure 5C). Interestingly, a considerable accumulation of $p27^{Kip1}$ was detected in SKRC-17 cells transfected with siRNA against *Notch-1* compared with control-transfected cells (Figure 5C), an experimental approach that, in contrast to treatment with DAPT, led to considerable inhibition of cell-cycle progression. Furthermore, in SKRC-52 cells transfected with siRNA against *Notch-1*, a substantial accumulation of $p21^{Cip1}$ could be observed compared with cells transfected with control siRNA (Figure 5C). We also analyzed the effect of siRNA against *Jagged-1* on proliferation. Western blot experiments verified the efficacy of this siRNA (Figure 5D). No effect on proliferation could, however, be detected upon *Jagged-1* ablation (Figure 5E). We therefore conclude that the growth-promoting effect of Notch signaling in CCRCC cells can be specifically attributed to the Notch-1 receptor.

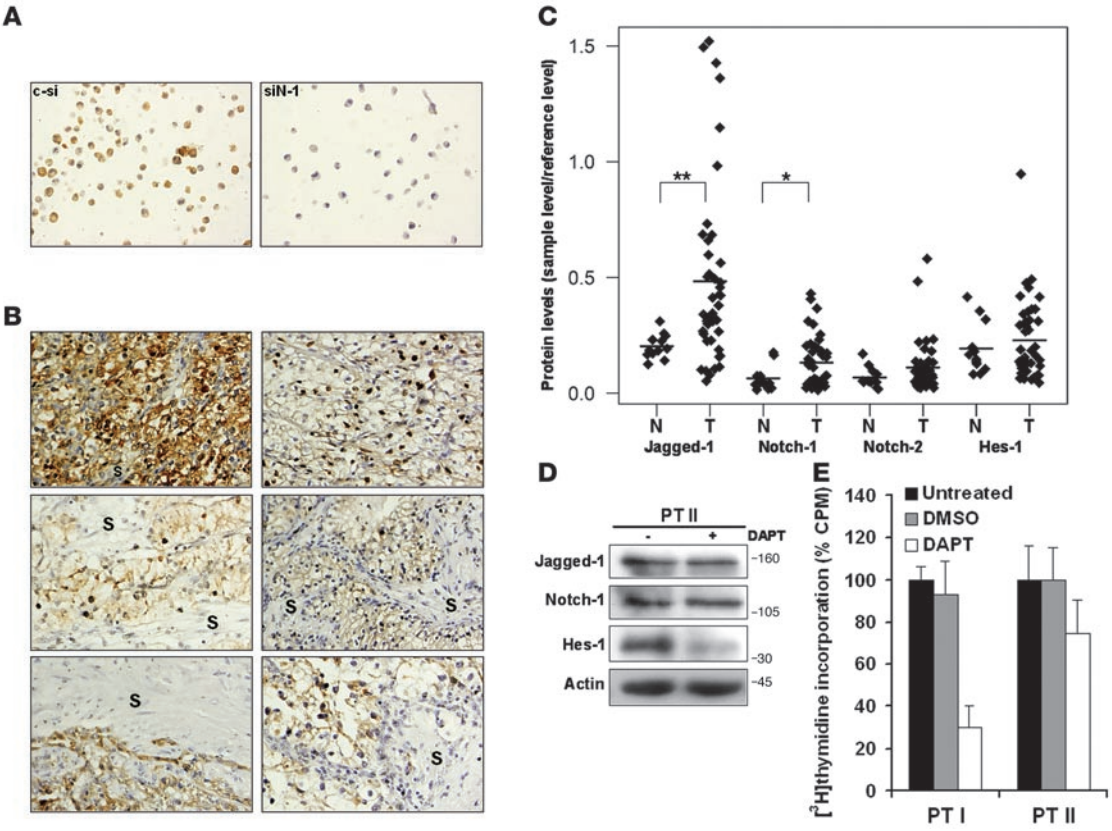

Figure 6

Notch pathway components are expressed in primary CCRCCs, and Notch inhibition restrains growth of freshly isolated CCRCC cells. (**A**) Immunohistochemistry of Notch-1 expression in SKRC-7 cells transfected with control siRNA or siRNA against *Notch-1* (siN-1). Original magnification, ×40. (**B**) Immunohistochemical assessment of Notch-1 expression in 6 CCRCC tumors and adjacent stromata (S). Original magnification, ×40. (**C**) Lysates from 43 primary CCRCCs (T) and 12 normal kidneys (N) were analyzed for Jagged-1, Notch-1, Notch-2, and Hes-1 expression by Western blot analyses. Results were normalized relative to the amount of actin and were plotted by the amount relative to reference sample. $^{*}P < 0.05$; $^{**}P < 0.01$, statistically significant changes (T versus N). Bonferroni's correction was used to adjust for multiple comparisons. (**D**) Primary CCRCC cell lysates were analyzed by immunoblotting for Jagged-1, Notch-1, and Hes-1 protein expression. Cells (PT II) were harvested after 24 hours of DAPT (+) and vehicle control (–) treatment. (**E**) CCRCC cells (PT I and PT II) isolated from 2 patients were analyzed by [^{3}H]thymidine incorporation. The cells were treated for 72 hours with DMSO or DAPT or left untreated (100%). Bars represent mean + SD of 1 experiment performed with each treatment 6 times.

Notch pathway elements are overexpressed in primary CCRCCs, and Notch inhibition suppresses growth of freshly isolated CCRCC cells. Our experimental data showed that the Notch cascade is expressed and active in CCRCC cell lines. This prompted us to investigate the expression of Notch pathway elements in primary CCRCCs. To show that Notch-1 is expressed in CCRCC tumor cells, we performed immunohistochemistry against Notch-1. In order to verify the specificity of the Notch-1 antibody, the staining patterns in paraffin-embedded SKRC-7 cells transfected with siRNA against *Notch-1* or control siRNA were analyzed. As shown in Figure 6A, Notch-1 staining could readily be detected in the control cells, while the staining intensity was dramatically reduced in cells transfected with siRNA against *Notch-1*. Six primary tumor samples were thereafter analyzed and Notch-1 expression was only detected in tumor cells, while the tumor stroma was Notch-1 negative (Figure 6B). In 2 of the tumors, Notch-1 staining could be detected in the nuclear region of the tumor cells, which is indicative of highly active Notch-1 signaling (Figure 6B). In order to more accurately quantitate Notch pathway expression in primary CCRCCs, we assessed Notch-1, Notch-2, Jagged-1, and Hes-1 levels using Western blots in a larger collection of samples, including 43 CCRCCs and 12 normal kidney extracts. The mean expression levels of all analyzed proteins were higher in tumor-derived extracts compared with normal control samples (Figure 6C). However, after Bonferroni's post-hoc correction, only Notch-1 and Jagged-1 were significantly elevated in CCRCCs. To provide firmer support for the presence and function of the Notch signaling pathway in CCRCC, we isolated CCRCC cells from 2 primary tumors. Western blot experiments using extracts from one of these short-term cultures confirmed as anticipated that primary CCRCC cells expressed Notch-1, Jagged-1, and Hes-1 proteins (Figure 6D). When treating these cells with DAPT, a substantial decrease in Hes-1 expression could be detected, showing that the Notch pathway is constitutively active also in primary CCRCC cells (Figure 6D). In analogy with the biological response of established CCRCC cell lines to Notch inhibition, a decrease in proliferation could be detected in primary CCRCC cells treated with DAPT compared with control cells (Figure 6E). Taken together, our data indicate that the expres-

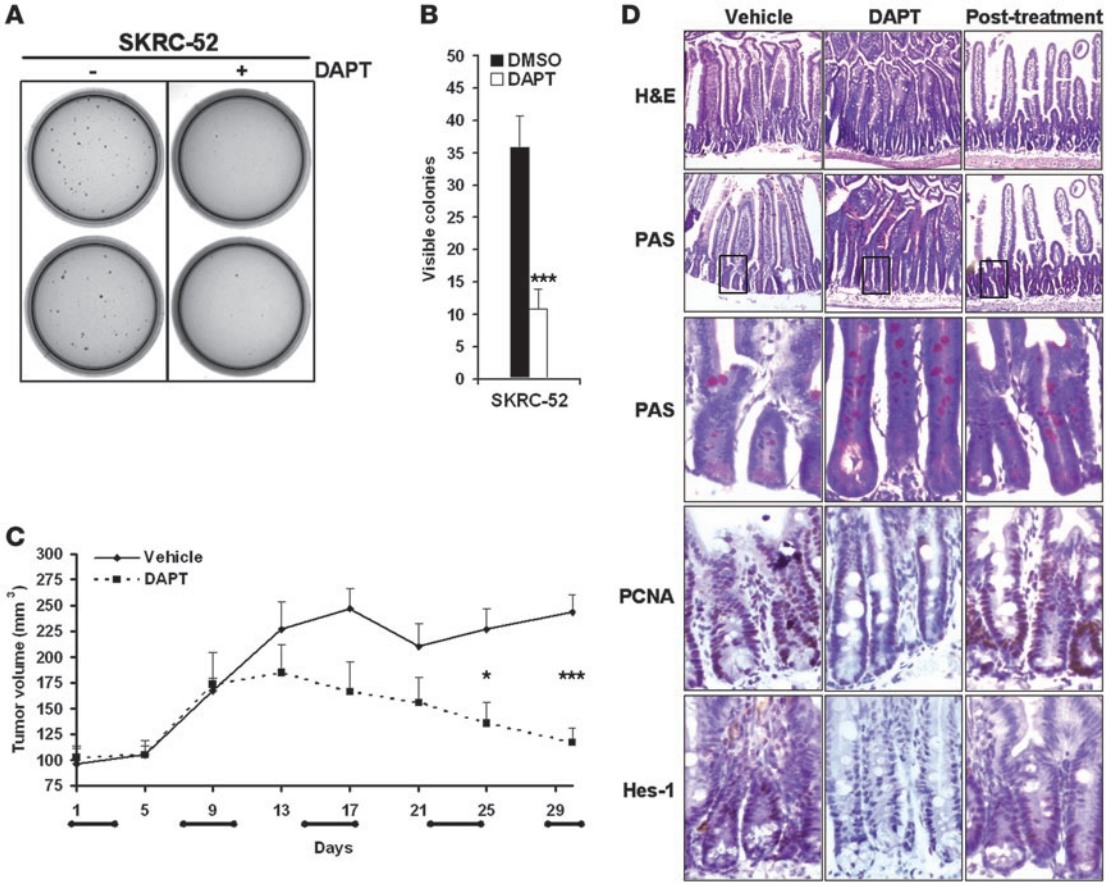

Figure 7

γ-Secretase treatment limits anchorage-independent growth and attenuates tumor growth in vivo. (**A** and **B**) The effect of DAPT (+) treatment on anchorage-independent growth of SKRC-52 cells compared with vehicle control (–) treatment. Cells were plated in soft agar and were cultured for 30 days with DMSO or DAPT. Results are shown as representative experiment (**A**) or mean + SD of 3 experiments (**B**), each performed in triplicate. ***$P < 0.001$, statistically significant changes (DAPT versus DMSO). (**C**) Growth of SKRC-52 xenografts in nude mice treated with DAPT (10 mg/kg/day) or vehicle control. Animals were treated in cycles of 3 days (horizontal bars on *x* axis), with daily injections followed by 4 days without treatment. Data represent the mean tumor volume (mm^3) + SEM of DAPT-treated ($n = 6$) or vehicle-treated ($n = 10$) mice. *$P < 0.05$; ***$P < 0.001$, statistically significant changes (DAPT versus vehicle). (**D**) Perturbed intestinal homeostasis induced by γ-secretase inhibition is partially normalized after 4 days without treatment. Immunohistochemical analyses of small intestines from vehicle control– and DAPT-treated mice after 48 hours of treatment or after a 4-day recovery period (after treatment). Representative sections of small intestine were stained with H&E or PAS or immunolabeled with PCNA and Hes-1 antibodies. Magenta/pink PAS staining indicates goblet cells and carbohydrate-rich mucin, whereas brown staining indicates PCNA and Hes-1 expression. Original magnification, ×10. Boxed areas of respective PAS staining were enlarged and displayed in the subsequent panel.

sion of Notch-1 and Jagged-1 are significantly elevated in primary CCRCCs and that inhibition of the pathway blocks growth of freshly isolated CCRCC cells.

DAPT treatment inhibits anchorage-independent growth of CCRCC cells and restrains growth of CCRCC cells in a xenograft tumor model. Anchorage-independent growth represents a hallmark feature of malignant cells, and to elucidate whether Notch inhibition impaired this capacity, we performed clonogenic assays of SKRC-52 cells treated with DAPT. A remarkable effect on clonogenicity was detected, with a 70% decrease upon DAPT treatment compared with vehicle control treatment (Figure 7, A and B).

We next wanted to clarify whether γ-secretase inhibition could restrain CCRCC growth in vivo. SKRC-52 cells were injected s.c. into nude mice, and animals were treated for 4 weeks with DAPT or vehicle control. A significant decrease in tumor growth could be detected in animals treated with DAPT in cycles with 3 days of daily injections and 4 days without treatment (Figure 7C). It is known that chronic treatment with γ-secretase inhibitors causes massive expansion of goblet cells in the crypt compartment due to the central role of Notch signaling in fate selection of crypt progenitor cells (41–43). We therefore also analyzed the small intestines of mice treated with intermittent DAPT dosing using immunohistochemistry. After 48 hours of treatment in the final dosing period, the villi were modestly runted and the crypt compartment was clearly elongated in DAPT-treated mice compared with control animals (Figure 7D). PAS staining indicated an expansion of goblet cells and an accumulation of intraluminal mucus in Notch-inhibited mice. We also noted a decreased expression of Hes-1 in the transient amplifying cell pool upon Notch inhibition. This was accompanied by a modest decrease in proliferation in treated animals compared with control animals, as indicated by decreased proliferating cell nuclear antigen (PCNA) staining (Figure 7D).

Together, these results most likely reflect a DAPT-induced partial conversion of the proliferating precursor cell pool into postmitotic goblet cells, albeit with a much less profound phenotypic conversion compared with previously published protocols using chronic administration of γ-secretase inhibitors (42, 43). Interestingly, 96 hours after treatment, the gross morphology and expression of PCNA and Hes-1 in the transient amplifying compartment showed clear signs of recovery, though the number of goblet cells and hence mucin remained slightly elevated compared with control animals (Figure 7D). These results indicate that the intermittent treatment regime employed in this study would allow for a partial recovery of the small intestine between the successive rounds of drug delivery. This conclusion was substantiated by our observation that the mice maintained their weight during the course of the experiment (Supplemental Figure 2), as weight loss is a principal side effect associated with chronic treatment with γ-secretase inhibitors (43).

Further studies are, however, required to fully delineate the optimal therapeutic administration regime in order to maximize the antitumorigenic effects without interfering with the normal function of Notch signaling in regenerating tissues.

Discussion

The role of Notch signaling in CCRCC has, to our knowledge, not been experimentally assessed previously, though *Notch-3* and *Jagged-1* mRNAs were reported to be elevated in CCRCC (44, 45). In this study, we show that the cardinal components of the Notch cascade were expressed in CCRCC cell lines. Likewise, in primary CCRCCs, we detected expression of Notch pathway proteins, with significantly higher levels of Notch-1 and Jagged-1 compared with normal kidney. Treatment of CCRCC cells with the Notch inhibitor DAPT led to a considerable decrease of Hes-1 in all but 1 cell line tested and in freshly isolated primary tumor cells, suggesting that active Notch signaling is an inherent property of CCRCC cells. Importantly, we could also show that inhibition of Notch signaling attenuates growth of CCRCC cells both in vitro and in vivo. It should be noted that the experimental data presented in this study were obtained by modulating endogenous Notch signaling, thus avoiding the pitfalls of supraphysiological levels often accomplished when exogenous icNotch is introduced. For example, in CNS stem cells, low levels of icNotch-1 promote growth whereas high levels induce growth arrest (46).

γ-Secretase inhibitors are valuable tools for delineating the cell biological function of the Notch cascade, but since they affect all Notch receptor paralogs, our experiments did not specify the individual contributions of the respective receptors. Furthermore, γ-secretase might affect other proteins involved in proliferation control (40). However, since ablation of *Notch-1* using siRNA led to decreased proliferation, we conclude that this Notch receptor is the critical target for the antiproliferative effect of γ-secretase inhibition in CCRCC cells. When targeting Jagged-1, no effect on proliferation could be detected, indicating that Notch receptor activation in vitro is not a consequence of autocrine or paracrine activation of the Notch-1 receptor by Jagged-1. However, in primary tumor specimens, Jagged-1 expression was significantly elevated compared with normal kidney, implying a potential involvement in other aspects of tumorigenic growth. For example, in head and neck squamous carcinoma, elevated Jagged-1 expression, as a consequence of RAS/MAPK activation, was shown to activate Notch receptors on tumor-infiltrating endothelial cells and thereby promote angiogenesis (47). Interestingly, the SKRC-17 cells that were refractory to γ-secretase treatment displayed a robust decline in proliferation upon ablation of *Notch-1* expression. How these cells escape inhibition of γ-secretase cleavage remains to be determined. It should be noted that some T cell acute lymphoblastic leukemia cells harboring *Notch-1*–activating mutations also were refractory to γ-secretase treatment (18). Recent data show that mutations of *FBW7*, a ubiquitin ligase involved in degradation of icNotch, render these cells refractory to pharmacological inhibitors (48). It will be important to clarify whether mutations in the Notch pathway are present in a subset of CCRCCs.

The regulatory effect of Notch signaling on $p21^{Cip1}$ and $p27^{Kip1}$, 2 CDK inhibitory proteins of pivotal importance in cell-cycle control, seems to be one important determinant for the cell type–specific effects of Notch signaling. In cell types in which Notch signaling is growth inhibiting, such as keratinocytes and small cell lung cancer cells, induced Notch signaling leads to upregulation of $p21^{Cip1}$ and/or $p27^{Kip1}$ (49, 50). In other cell types, such as endothelial and pancreatic cancer cells, high Notch activity is associated with decreased expression of $p21^{Cip1}$ and/or $p27^{Kip1}$ (38, 39). Our data suggest that elevation of $p21^{Cip1}$ and $p27^{Kip1}$ might represent a potential mechanism for the growth-restraining effect of Notch inhibition in CCRCC cells. It is noteworthy that in CCRCC, low $p27^{Kip1}$ expression has been associated with unfavorable prognosis (51, 52). Further studies are required to determine the molecular link between $p21^{Cip1}$ and $p27^{Kip1}$ regulation and Notch signaling in CCRCC cells.

Due to the loss of *VHL* and hence constitutive activation of HIF-1α and, in particular, HIF-2α, CCRCC tumors are characterized by an oxygen-independent hypoxic response. The loss of *VHL* is an early event in the genesis of CCRCC and is considered to be associated with a gatekeeper function of the tumor suppressor gene, i.e., *VHL* loss is a prerequisite for tumor formation, but additional oncogenic events affecting other aspects of the tumorigenic process are most likely involved in tumor progression (12). We have previously reported that Notch signaling is elevated in hypoxic human neuroblastoma cells (27, 28). Recently, it was shown that differentiation of neuronal and muscle progenitor cells was inhibited by hypoxia in a Notch signaling–dependent manner, and a physical interaction between HIF-1α and icNotch-1, which potentiated activation of Notch target genes, was reported (26). Since our data clearly showed that Notch signaling activity in CCRCC cells was not suppressed by pVHL restoration or HIF-α knockdown and not enhanced by hypoxia, we consider it unlikely that the VHL/HIF pathway augments Notch signaling in CCRCC cells. On the contrary, a slight increase in primary downstream target genes could, for unknown reasons, be detected in the pVHL-reconstituted CCRCC cells. However, since an almost complete downregulation of Hes-1 could be detected upon γ-secretase treatment irrespective of the pVHL status of the cells, we conclude that the γ-secretase responsiveness is not associated with the VHL/HIF axis.

Until recently, no efficient treatment for metastatic CCRCC was available. However, several kinase inhibitors, e.g., sorafenib and sunitinib, show substantial effects on progression-free survival for patients with adverse disease (2, 3). The efficacy of these drugs most likely relates to their capacity to inhibit HIF-mediated autocrine growth factor signaling and proangiogenic effects. Interestingly, loss of *VHL* is associated with good prognosis in CCRCC (53, 54). The therapeutic effect of γ-secretase inhibition on CCRCC tumor growth indicates that inhibition of Notch signaling might represent a complementary therapeutic approach for treatment of

CCRCC. However, it is well known that in vivo use of γ-secretase inhibitors is associated with considerable adverse effects (43, 55). In particular, intestinal differentiation is perturbed due to massive expansion of goblet cells (41, 42). Our intermittent administration regime decreased the adverse effects on the rapidly turned over crypt cells while the cytostatic effect on the tumors was maintained. A comprehensive evaluation of the optimal administration regime of γ-secretase inhibitors is therefore of high priority. It should be noted that histopathological analyses revealed no adverse effects on normal kidney in long-term treatment of mice with γ-secretase inhibitors in a previous study (43). In addition, we noticed a striking inhibition of clonogenicity in soft agar experiments when CCRCC cells were treated with DAPT. It will be important to clarify whether the general effects on proliferation might be associated with a depletion of tumor-initiating cells, an effect of Notch inhibition that has been observed in other tumors, such as medulloblastoma (56).

Several recent studies unequivocally show that Notch signaling is pivotal for tumor angiogenesis (57–60). The Notch ligand Dll-4 seems to be essential for tumor angiogenesis, and thus, Dll-4 inhibition is emerging as a promising antiangiogenic therapeutic approach. Importantly, the expression of Dll-4 is particularly high in endothelial cells in the richly vascularized CCRCC tumors (38). However, based on the results presented in this study, we speculate that global targeting of the Notch pathway in CCRCC might be particularly efficient, since it might serve a dual purpose by affecting the growth capacity of the tumor cells and at the same time impeding angiogenesis.

Methods

Cell culture and reagents. The CCRCC cell line 786-O was obtained from ATCC and maintained in DMEM (Invitrogen) supplemented with 10% FCS and 1% penicillin/streptomycin (PEST). 786-O subclones stably transfected with either pRc/CMV (PRC3) or pRc/CMV-HA-VHL (WT7) were generous gifts from W.G. Kaelin Jr. (Dana-Farber Cancer Institute and Brigham and Women's Hospital, Harvard Medical School, Boston, USA) (4) and were maintained as above with the addition of 1 mg/ml G418 (GIBCO; Invitrogen). The CCRCC cell lines SKRC-7, SKRC-10, SKRC-17, and SKRC-21 (29, 31) were kindly provided by E. Oosterwijk (Radboud University Nijmegen Medical Center, Nijmegen, The Netherlands) and maintained in RPMI 1640 (Invitrogen) containing 10% FCS and PEST. The CCRCC cell lines SKRC-52 and Caki-2 were maintained in RPMI 1640 as above. The primary tumor cells (PT I and PT II) were derived from primary lesions provided with informed consent by 2 patients who had undergone radical nephrectomy at University Hospital MAS. The primary lesions were histopathologically verified as CCRCCs. After surgery, tumor tissue fragments were processed by enzymatic digestion, and tumor cells were maintained in high-glucose DMEM (Invitrogen) supplemented with 10% FCS and PEST. Cells were treated with indicated concentrations of the γ-secretase inhibitor DAPT (Calbiochem) or 5 μM L-685458 (Bachem) or the corresponding volume of the vehicle DMSO for indicated times.

siRNA and hypoxia experiments. Cells were seeded in 60-mm plates 24 hours prior to siRNA transfection. Cells were then transfected with control siRNA or siRNA against *HIF-1α* or *HIF-2α* (Ambion) or siRNA against *Notch-1*, *Notch-2*, or *Jagged-1* (Santa Cruz Biotechnology Inc.) using Lipofectamine 2000 (Invitrogen) for 6 or 24 hours in OptiMEM I Reduced Serum Medium (Invitrogen). Cells were harvested at indicated time points. In hypoxia experiments, cells were grown at 1% O_2 in a 400 Hypoxia Workstation (Ruskinn Technology Ltd.) connected to a Ruskinn gas mixer module.

Western blot and Q-PCR analyses. Cells were lysed in RIPA buffer, separated on an SDS-PAGE gel, and blotted onto Immobilon-P (Millipore) or Hybond-C (Amersham) membranes. Antibodies are provided in Supplemental Methods. Western blot experiments were performed at least 3 times.

Total RNA extraction and quantification of gene expression using SYBR Green (Applied Biosystems) were performed as described previously (61). The relative quantification of mRNA was done using the comparative C^t method and normalized to 3 endogenous reference genes, succinate dehydrogenase complex subunit A (*SDHA*), tyrosine 3-monooxygenase/tryptophan 5-monooxygenase activation protein (*YWHAZ*), and ubiquitin C (*UBC*) (62). Primer sequences are given in Supplemental Table 1. The experiments were repeated twice and the data shown as mean + SD of representative experiments, performed in triplicate.

Thymidine incorporation assays. In γ-secretase inhibition experiments, 5.0×10^4 cells were seeded in 96-well plates in 200 μl 1% FCS–supplemented media or 1% FCS media supplemented with DMSO or DAPT and incubated for 72 hours. [^{3}H]thymidine (Amersham Life Sciences) was then added to the culture. Cells were harvested after 24 hours, and the incorporated [^{3}H]thymidine was measured as counts per minute in a β-liquid scintillation counter (LKB RackBeta Wallace). Each experiment was performed 6 times and repeated 3 times. In siRNA experiments, cells were seeded in 60-mm plates 24 hours prior to transfection. The cells were then transfected with siRNA as indicated above, after which 5.0×10^4 cells were reseeded in 96-well plates in 200 μl 1% FCS–supplemented media and incubated for 72 hours whereafter [^{3}H]thymidine incorporation was assessed as above.

Cell counting and TB exclusion assays. 7.0×10^4 cells were seeded in 60-mm plates 1 day prior to initiation of experiment. Starting at day 0, cells were trypsinized and stained with 0.4% TB solution (Sigma-Aldrich), and both viable and dead cells were counted in a Bürker chamber. Every other day, starting at day 0, cultures for subsequent counting were supplemented with fresh media containing 1% FCS, PEST, and DMSO or DAPT. Each experiment was performed in triplicate and repeated twice.

Flow cytometric analyses. For cell-cycle distribution experiments, cells were synchronized with serum-free medium for 24 hours and then supplemented with fresh medium containing 1% FCS, PEST, and DMSO or DAPT for 24 hours. Cells were harvested by centrifugation, resuspended in 70% ethanol, and stored at –20°C. Cells were washed in cold PBS, after which 800 μl Vindelöv solution was added to the cells and left to incubate for 20 minutes on ice. DNA analyses were performed using a FACSCalibur flow cytometer (BD), and the fraction of sub-G_1, G_0G_1, S, and G_2M cells was determined using CellQuest 3.2 software (BD). Each experiment was performed in triplicate and repeated 3 times.

Analyses of primary tumors. Tumor samples collected at the University Hospital in Umeå, Sweden, including 6 nephrectomy specimens from 6 patients, were analyzed by immunohistochemistry. The tumors were classified as CCRCCs according to the Heidelberg classification system (63). All tumor samples were obtained after permission from the patients with informed and signed consent, and the study was approved by the Institutional Review Board. Paraffin sections (4 μm) from the paraffin-embedded tissue specimens were deparaffinized and microwave treated according to standard procedures. After antigen retrieval, Notch-1 (Santa Cruz Biotechnology Inc.) immunoreactivity was detected using the Dako EnVision system and Dako TechMate 500. Sections were counterstained with H&E. To evaluate antibody specificity, Notch-1 immunoreactivity of siRNA control-transfected SKRC-7 cells or SKRC-7 cells in which the antigen had been eliminated by siRNA against *Notch-1* was performed. Immunohistochemistry of SKRC-7 cells were performed as described above.

Preparation of protein extracts from fresh-frozen tissues was performed as described earlier (51). Protein extract from each sample and a positive control (SKRC-52) were separated on SDS-PAGE, and immunoblotting

was performed as described above. The amount of protein in each sample was determined by densitometry (ImageJ software, v. 1.34) and normalized to the amount of actin and positive control.

Anchorage-independent growth analyses. 1.5×10^4 SKRC-52 cells were resuspended in 1% FCS RPMI 1640 medium containing 0.7% agarose and DMSO or DAPT. This suspension was layered over a 0.5% agar medium base layer in 60-mm plates and treated with DMSO or DAPT every second day for a total of 30 days, whereafter macroscopically visible colonies were counted. Each experiment was performed in triplicate and repeated 3 times.

Xenograft tumor model. 2.0×10^6 SKRC-52 cells in 100 μl of PBS were injected s.c. into the flank of 6- to 8-week-old athymic female mice (NMRI strain nu/nu; Taconic). Tumor volume was determined as $\pi ls^2/6$, where l = long side and s = short side. When the tumor volumes reached approximately 100 mm^3, mice were treated s.c. with 100 μl vehicle control (10% ethanol, 90% corn oil) or 10 mg/kg DAPT (dissolved in 10% ethanol, 90% corn oil) as previously described (57). A regime of daily treatment was continued for 3 days followed by 4 days without treatment. This treatment regime was repeated 5 times. At the end of the dosing period, animals were sacrificed and small intestines of 3 DAPT- and 3 vehicle-treated mice were collected for histological analyses. Samples were also collected from 3 DAPT-treated mice 4 days after the final dosing. Formalin-fixed tissues were prepared as described above. Sections were stained with PAS in order to visualize carbohydrate-rich mucin. Immunoreactivity was analyzed as above using a PCNA antibody (Dako) or Hes-1 antiserum kindly provided by T. Sudo (Toray Industries Inc., Kamakura, Japan). All animal experiments were approved by the Malmö/Lund ethical committee, Lund, Sweden (approval no. M24–07).

Statistics. Statistical analyses were performed using 2-tailed Student's *t* test. Bonferroni's correction was used to adjust for multiple comparisons in analyses of primary tumor samples.

Acknowledgments

We are grateful to W.G. Kaelin Jr. for providing the PRC3 and WT7 cells; E. Oosterwijk for providing SKRC-7, SKRC-10, SKRC-17, and SKRC-21 cells; and T. Sudo for generously providing the Hes-1 antiserum. We are also grateful to M. Hellström for advice regarding the preparation of DAPT for the in vivo experiments and to E. Fredlund for statistical advice. This work was supported by grants from the Swedish Cancer Society, the Children's Cancer Foundation of Sweden, Åke Wiberg's Foundation, Ollie and Elof Ericsson's Foundation, the Crafoord Foundation, Gunnar Nilsson's Cancer Foundation, and Malmö University Hospital research funds.

Received for publication March 9, 2007, and accepted in revised form October 17, 2007.

Address correspondence to: Håkan Axelson, Center for Molecular Pathology, Department of Laboratory Medicine, Lund University, University Hospital MAS, Entrance 78, SE-205 02 Malmö, Sweden. Phone: 46-40337621; Fax: 46-40337063; E-mail: hakan.axelson@med.lu.se.

1. Zbar, B., Klausner, R., and Linehan, W.M. 2003. Studying cancer families to identify kidney cancer genes. *Annu. Rev. Med.* **54**:217–233.
2. Escudier, B., et al. 2007. Sorafenib in advanced clear-cell renal-cell carcinoma. *N. Engl. J. Med.* **356**:125–134.
3. Motzer, R.J., et al. 2007. Sunitinib versus interferon alfa in metastatic renal-cell carcinoma. *N. Engl. J. Med.* **356**:115–124.
4. Iliopoulos, O., Kibel, A., Gray, S., and Kaelin, W.G., Jr. 1995. Tumour suppression by the human von Hippel-Lindau gene product. *Nat. Med.* **1**:822–826.
5. Kondo, K., Klco, J., Nakamura, E., Lechpammer, M., and Kaelin, W.G., Jr. 2002. Inhibition of HIF is necessary for tumor suppression by the von Hippel-Lindau protein. *Cancer Cell.* **1**:237–246.
6. Maranchie, J.K., et al. 2002. The contribution of VHL substrate binding and HIF1-alpha to the phenotype of VHL loss in renal cell carcinoma. *Cancer Cell.* **1**:247–255.
7. Maxwell, P.H., et al. 1999. The tumour suppressor protein VHL targets hypoxia-inducible factors for oxygen-dependent proteolysis. *Nature.* **399**:271–275.
8. Semenza, G.L. 2003. Targeting HIF-1 for cancer therapy. *Nat. Rev. Cancer.* **3**:721–732.
9. Gordan, J.D., Bertout, J.A., Hu, C.J., Diehl, J.A., and Simon, M.C. 2007. HIF-2alpha promotes hypoxic cell proliferation by enhancing c-myc transcriptional activity. *Cancer Cell.* **11**:335–347.
10. Raval, R.R., et al. 2005. Contrasting properties of hypoxia-inducible factor 1 (HIF-1) and HIF-2 in von Hippel-Lindau-associated renal cell carcinoma. *Mol. Cell. Biol.* **25**:5675–5686.
11. Yan, Q., Bartz, S., Mao, M., Li, L., and Kaelin, W.G., Jr. 2007. The hypoxia-inducible factor 2alpha N-terminal and C-terminal transactivation domains cooperate to promote renal tumorigenesis in vivo. *Mol. Cell. Biol.* **27**:2092–2102.
12. Kim, W.Y., and Kaelin, W.G. 2004. Role of VHL gene mutation in human cancer. *J. Clin. Oncol.* **22**:4991–5004.
13. Seagroves, T., and Johnson, R.S. 2002. Two HIFs may be better than one. *Cancer Cell.* **1**:211–213.
14. Artavanis-Tsakonas, S., Rand, M.D., and Lake, R.J. 1999. Notch signaling: cell fate control and signal integration in development. *Science.* **284**:770–776.
15. Hansson, E.M., Lendahl, U., and Chapman, G. 2004. Notch signaling in development and disease. *Semin. Cancer Biol.* **14**:320–328.
16. Iso, T., Kedes, L., and Hamamori, Y. 2003. HES and HERP families: multiple effectors of the Notch signaling pathway. *J. Cell. Physiol.* **194**:237–255.
17. Ellisen, L.W., et al. 1991. TAN-1, the human homolog of the Drosophila notch gene, is broken by chromosomal translocations in T lymphoblastic neoplasms. *Cell.* **66**:649–661.
18. Weng, A.P., et al. 2004. Activating mutations of NOTCH1 in human T cell acute lymphoblastic leukemia. *Science.* **306**:269–271.
19. Miele, L., Golde, T., and Osborne, B. 2006. Notch signaling in cancer. *Curr. Mol. Med.* **6**:905–918.
20. Sjolund, J., Manetopoulos, C., Stockhausen, M.T., and Axelson, H. 2005. The Notch pathway in cancer: differentiation gone awry. *Eur. J. Cancer.* **41**:2620–2629.
21. Chen, L., and Al-Awqati, Q. 2005. Segmental expression of Notch and Hairy genes in nephrogenesis. *Am. J. Physiol. Renal Physiol.* **288**:F939–F952.
22. Yu, J., McMahon, A.P., and Valerius, M.T. 2004. Recent genetic studies of mouse kidney development. *Curr. Opin. Genet. Dev.* **14**:550–557.
23. Zambrano, N.R., Lubensky, I.A., Merino, M.J., Linehan, W.M., and Walther, M.M. 1999. Histopathology and molecular genetics of renal tumors toward unification of a classification system. *J. Urol.* **162**:1246–1258.
24. Cheng, H.T., et al. 2007. Notch2, but not Notch1, is required for proximal fate acquisition in the mammalian nephron. *Development.* **134**:801–811.
25. McCright, B., et al. 2001. Defects in development of the kidney, heart and eye vasculature in mice homozygous for a hypomorphic Notch2 mutation. *Development.* **128**:491–502.
26. Gustafsson, M.V., et al. 2005. Hypoxia requires notch signaling to maintain the undifferentiated cell state. *Dev. Cell.* **9**:617–628.
27. Axelson, H., Fredlund, E., Ovenberger, M., Landberg, G., and Pahlman, S. 2005. Hypoxia-induced dedifferentiation of tumor cells--a mechanism behind heterogeneity and aggressiveness of solid tumors. *Semin. Cell Dev. Biol.* **16**:554–563.
28. Jogi, A., et al. 2002. Hypoxia alters gene expression in human neuroblastoma cells toward an immature and neural crest-like phenotype. *Proc. Natl. Acad. Sci. U. S. A.* **99**:7021–7026.
29. Grabmaier, K., et al. 2004. Strict regulation of CAIX(G250/MN) by HIF-1alpha in clear cell renal cell carcinoma. *Oncogene.* **23**:5624–5631.
30. Shinojima, T., et al. 2007. Renal cancer cells lacking hypoxia inducible factor (HIF)-1alpha expression maintain vascular endothelial growth factor expression through HIF-2alpha. *Carcinogenesis.* **28**:529–536.
31. Ebert, T., Bander, N.H., Finstad, C.L., Ramsawak, R.D., and Old, L.J. 1990. Establishment and characterization of human renal cancer and normal kidney cell lines. *Cancer Res.* **50**:5531–5536.
32. Mahon, P.C., Hirota, K., and Semenza, G.L. 2001. FIH-1: a novel protein that interacts with HIF-1alpha and VHL to mediate repression of HIF-1 transcriptional activity. *Genes Dev.* **15**:2675–2686.
33. Weinmaster, G., and Kopan, R. 2006. A garden of Notch-ly delights. *Development.* **133**:3277–3282.
34. Beverly, L.J., Felsher, D.W., and Capobianco, A.J. 2005. Suppression of p53 by Notch in lymphomagenesis: implications for initiation and regression. *Cancer Res.* **65**:7159–7168.
35. Klinakis, A., et al. 2006. Myc is a Notch1 transcriptional target and a requisite for Notch1-induced mammary tumorigenesis in mice. *Proc. Natl. Acad. Sci. U. S. A.* **103**:9262–9267.
36. Ronchini, C., and Capobianco, A.J. 2001. Induction of cyclin D1 transcription and CDK2 activity by Notch(ic): implication for cell cycle disruption in transformation by Notch(ic). *Mol. Cell. Biol.* **21**:5925–5934.
37. Sarmento, L.M., et al. 2005. Notch1 modulates timing of G1-S progression by inducing SKP2

transcription and p27 Kip1 degradation. *J. Exp. Med.* **202**:157–168.
38. Patel, N.S., et al. 2005. Up-regulation of delta-like 4 ligand in human tumor vasculature and the role of basal expression in endothelial cell function. *Cancer Res.* **65**:8690–8697.
39. Wang, Z., Zhang, Y., Li, Y., Banerjee, S., Liao, J., and Sarkar, F.H. 2006. Down-regulation of Notch-1 contributes to cell growth inhibition and apoptosis in pancreatic cancer cells. *Mol. Cancer Ther.* **5**:483–493.
40. Wolfe, M.S., and Kopan, R. 2004. Intramembrane proteolysis: theme and variations. *Science.* **305**:1119–1123.
41. Fre, S., et al. 2005. Notch signals control the fate of immature progenitor cells in the intestine. *Nature.* **435**:964–968.
42. van Es, J.H., et al. 2005. Notch/gamma-secretase inhibition turns proliferative cells in intestinal crypts and adenomas into goblet cells. *Nature.* **435**:959–963.
43. Wong, G.T., et al. 2004. Chronic treatment with the gamma-secretase inhibitor LY-411,575 inhibits beta-amyloid peptide production and alters lymphopoiesis and intestinal cell differentiation. *J. Biol. Chem.* **279**:12876–12882.
44. Rae, F.K., Stephenson, S.A., Nicol, D.L., and Clements, J.A. 2000. Novel association of a diverse range of genes with renal cell carcinoma as identified by differential display. *Int. J. Cancer.* **88**:726–732.
45. Zhao, H., et al. 2006. Gene expression profiling predicts survival in conventional renal cell carcinoma. *PLoS Med.* **3**:e13.
46. Guentchev, M., and McKay, R.D. 2006. Notch controls proliferation and differentiation of stem cells in a dose-dependent manner. *Eur. J. Neurosci.* **23**:2289–2296.
47. Zeng, Q., et al. 2005. Crosstalk between tumor and endothelial cells promotes tumor angiogenesis by MAPK activation of Notch signaling. *Cancer Cell.* **8**:13–23.
48. O'Neil, J., et al. 2007. FBW7 mutations in leukemic cells mediate NOTCH pathway activation and resistance to {gamma}-secretase inhibitors. *J. Exp. Med.* **204**:1813–1824.
49. Rangarajan, A., et al. 2001. Notch signaling is a direct determinant of keratinocyte growth arrest and entry into differentiation. *EMBO J.* **20**:3427–3436.
50. Sriuranpong, V., et al. 2001. Notch signaling induces cell cycle arrest in small cell lung cancer cells. *Cancer Res.* **61**:3200–3205.
51. Hedberg, Y., Ljungberg, B., Roos, G., and Landberg, G. 2003. Expression of cyclin D1, D3, E, and p27 in human renal cell carcinoma analysed by tissue microarray. *Br. J. Cancer.* **88**:1417–1423.
52. Langner, C., et al. 2004. Biological significance of p27 and Skp2 expression in renal cell carcinoma. A systematic analysis of primary and metastatic tumour tissues using a tissue microarray technique. *Virchows Arch.* **445**:631–636.
53. Banks, R.E., et al. 2006. Genetic and epigenetic analysis of von Hippel-Lindau (VHL) gene alterations and relationship with clinical variables in sporadic renal cancer. *Cancer Res.* **66**:2000–2011.
54. Yao, M., et al. 2002. VHL tumor suppressor gene alterations associated with good prognosis in sporadic clear-cell renal carcinoma. *J. Natl. Cancer Inst.* **94**:1569–1575.
55. Milano, J., et al. 2004. Modulation of notch processing by gamma-secretase inhibitors causes intestinal goblet cell metaplasia and induction of genes known to specify gut secretory lineage differentiation. *Toxicol. Sci.* **82**:341–358.
56. Fan, X., et al. 2006. Notch pathway inhibition depletes stem-like cells and blocks engraftment in embryonal brain tumors. *Cancer Res.* **66**:7445–7452.
57. Hellstrom, M., et al. 2007. Dll4 signalling through Notch1 regulates formation of tip cells during angiogenesis. *Nature.* **445**:776–780.
58. Noguera-Troise, I., et al. 2006. Blockade of Dll4 inhibits tumour growth by promoting non-productive angiogenesis. *Nature.* **444**:1032–1037.
59. Ridgway, J., et al. 2006. Inhibition of Dll4 signalling inhibits tumour growth by deregulating angiogenesis. *Nature.* **444**:1083–1087.
60. Siekmann, A.F., and Lawson, N.D. 2007. Notch signalling limits angiogenic cell behaviour in developing zebrafish arteries. *Nature.* **445**:781–784.
61. Stockhausen, M.T., Sjolund, J., Manetopoulos, C., and Axelson, H. 2005. Effects of the histone deacetylase inhibitor valproic acid on Notch signalling in human neuroblastoma cells. *Br. J. Cancer.* **92**:751–759.
62. Vandesompele, J., et al. 2002. Accurate normalization of real-time quantitative RT-PCR data by geometric averaging of multiple internal control genes. *Genome Biol.* **3**:research0034.1–research0034.11.
63. Kovacs, G., et al. 1997. The Heidelberg classification of renal cell tumours. *J. Pathol.* **183**:131–133.